Supplementary Information (SI) for Nanoscale.

Protein Structure and Bioactivity Upon Adsorption and Desorption from Nanosilicate Sustained Release Delivery Devices

Samuel Stealey [a], Ether Dharmesh [a], Akhilesh Gaharwar [b], Jai Rudra [c], Silviya P. Zustiak [a,*]

a) Department of Biomedical Engineering, Saint Louis University, St. Louis, MO

b) Department of Biomedical Engineering & Department of Materials Science and Engineering, College of Engineering, Texas A&M University, College Station, TX; Interdisciplinary Program in Genetics and Genomics, Texas A&M University, College Station, TX;

c) Department of Biomedical Engineering, Washington University in Saint Louis, St. Louis, MO

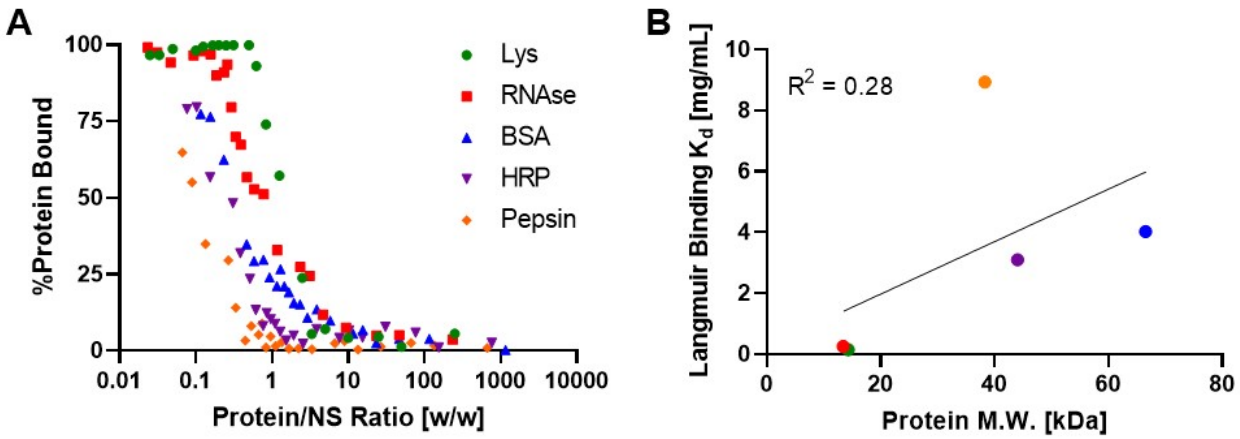

Supplemental Figure S1: A. Binding affinity showed similar trends when plotted against protein/NS mass ratio, indicating protein mass did not play a major role in determining affinity. **B.** Langmuir binding K_d did not show a clear correlation with protein molecular weight.

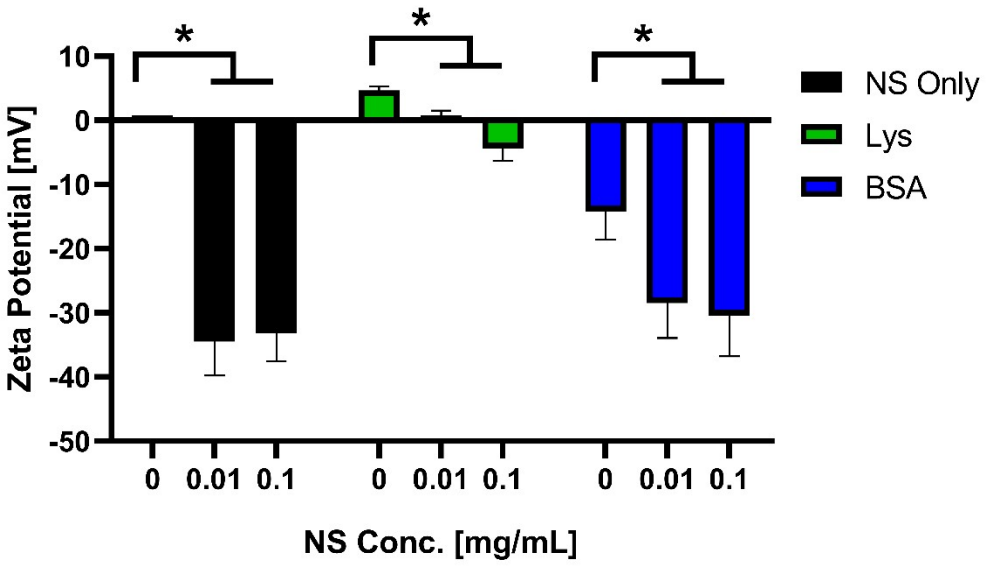

Supplemental Figure S2: Measured zeta potential of 1 mg/mL Lys or BSA with 0, 0.01, or 0.10 mg/mL NS. * indicates statistically significant difference between indicated groups ($N = 4$, $p < 0.05$).

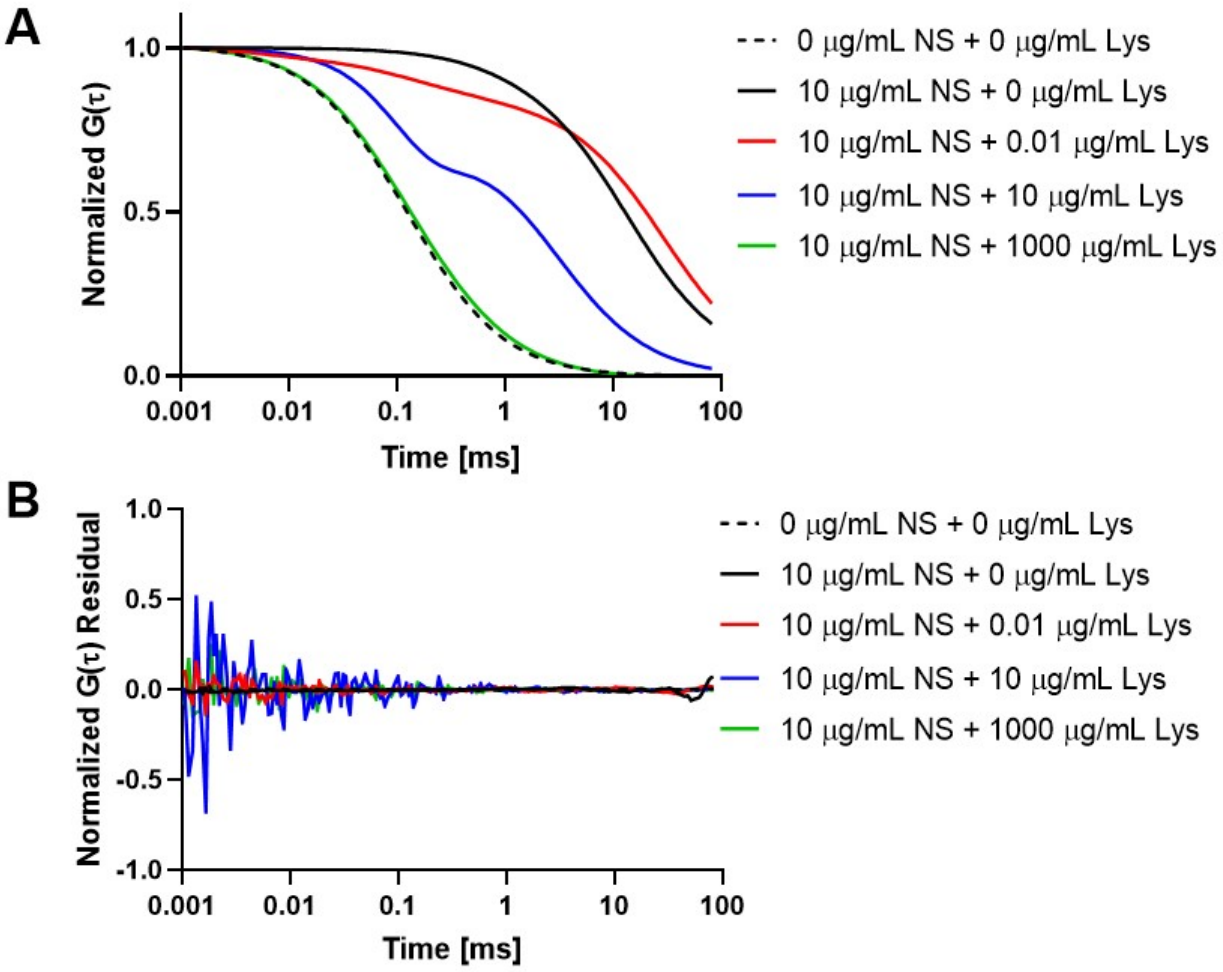

Supplemental Figure S3: A. Normalized autocorrelation curves of Atto-RNase (1 μg/mL) in the presence of varying concentrations of unlabeled Lys. **B.** Residuals of fitted curves from panel A showing the goodness of the fit.

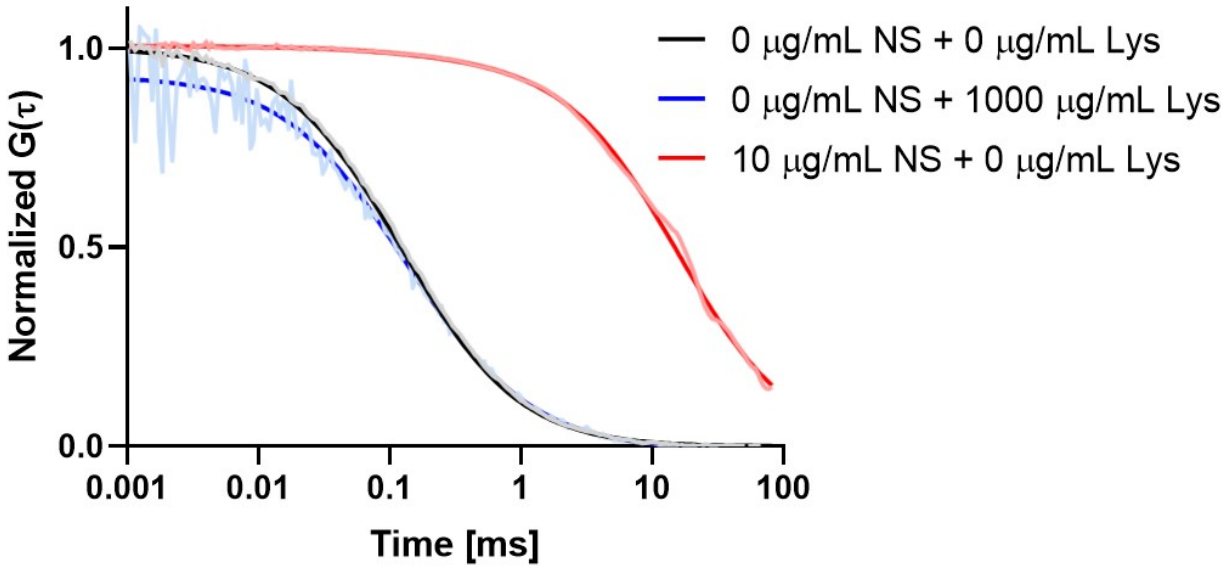

Supplemental Figure S4: Normalized autocorrelation curves of Atto-RNase A in the presence of unlabeled Lys with and without 10 μg/mL NS. Crowding due to high unlabeled protein concentration was shown not to have a significant effect on Atto-RNase A diffusivity, especially when compared to the effect of NS. Darker lines represent fitted autocorrelation curves, while lighter lines represent raw data.

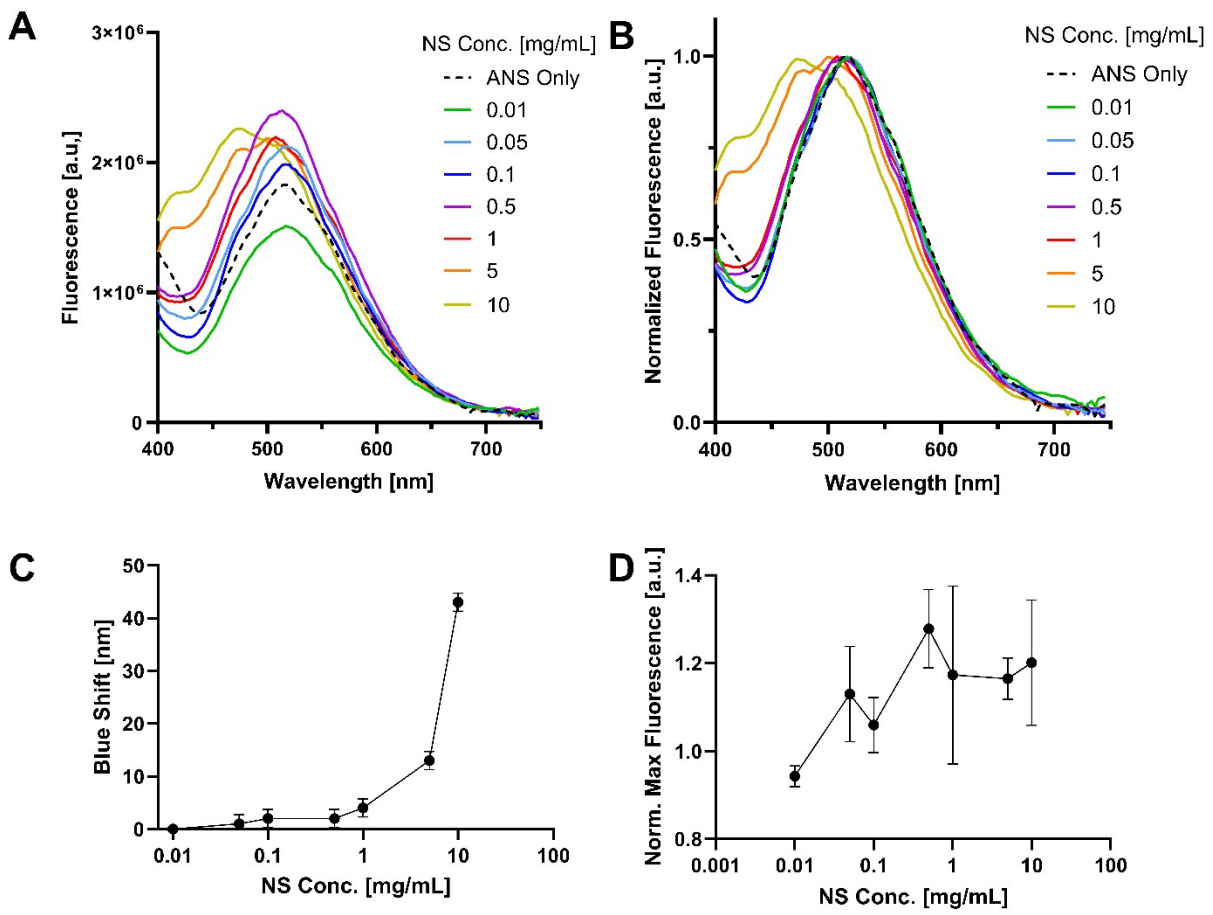

Supplemental Figure S5: Raw (**A**) and normalized (**B**) fluorescence curves of ANS in the presence of varying concentrations of NS and absence of protein. **C.** Blue shift of fluorescence maxima as a function of NS concentration. **D.** Effect of NS concentration on maximal fluorescence, normalized to the 0 mg/mL condition.

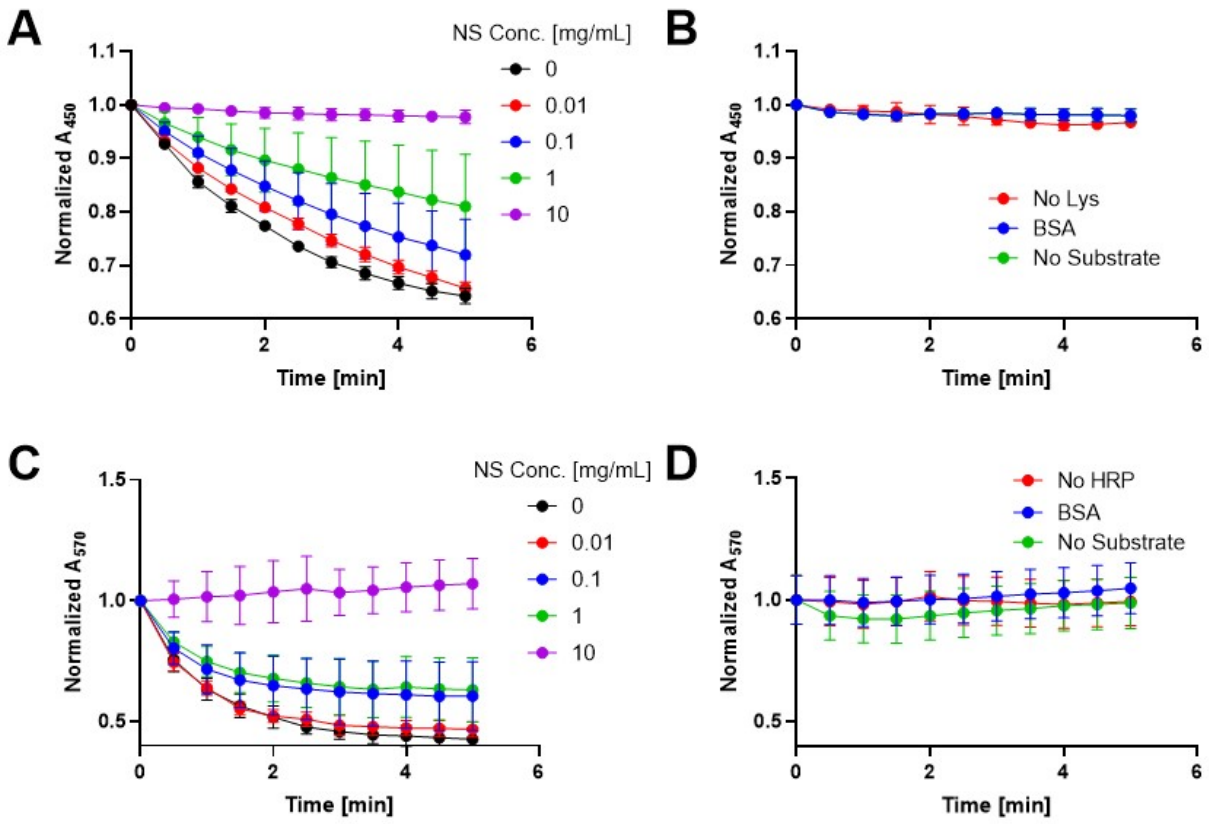

Supplemental Figure S6: A. Evolution of A_{450} of Lys activity assays with varying concentrations of NS and **(B)** associated negative controls. **C.** Evolution of A_{570} of HRP activity assays with varying concentrations of NS and **(D)** associated negative controls.

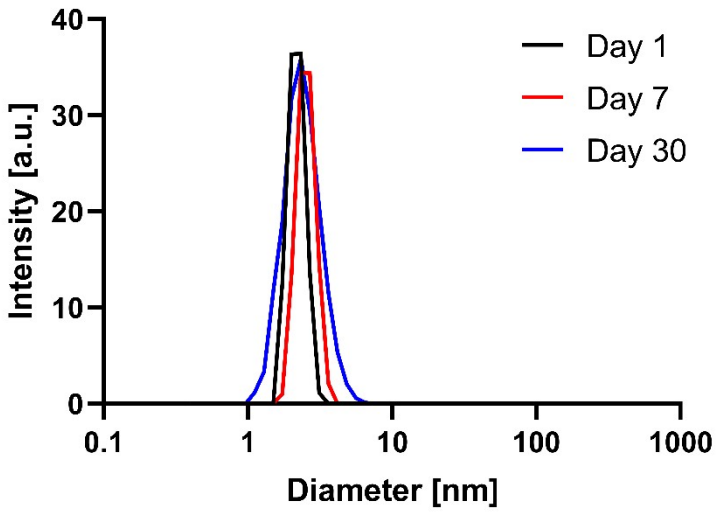

Supplemental Figure S7: DLS analysis of Lys released from PEG-NS hydrogels, revealing no significant protein aggregation or complexation in releasates.

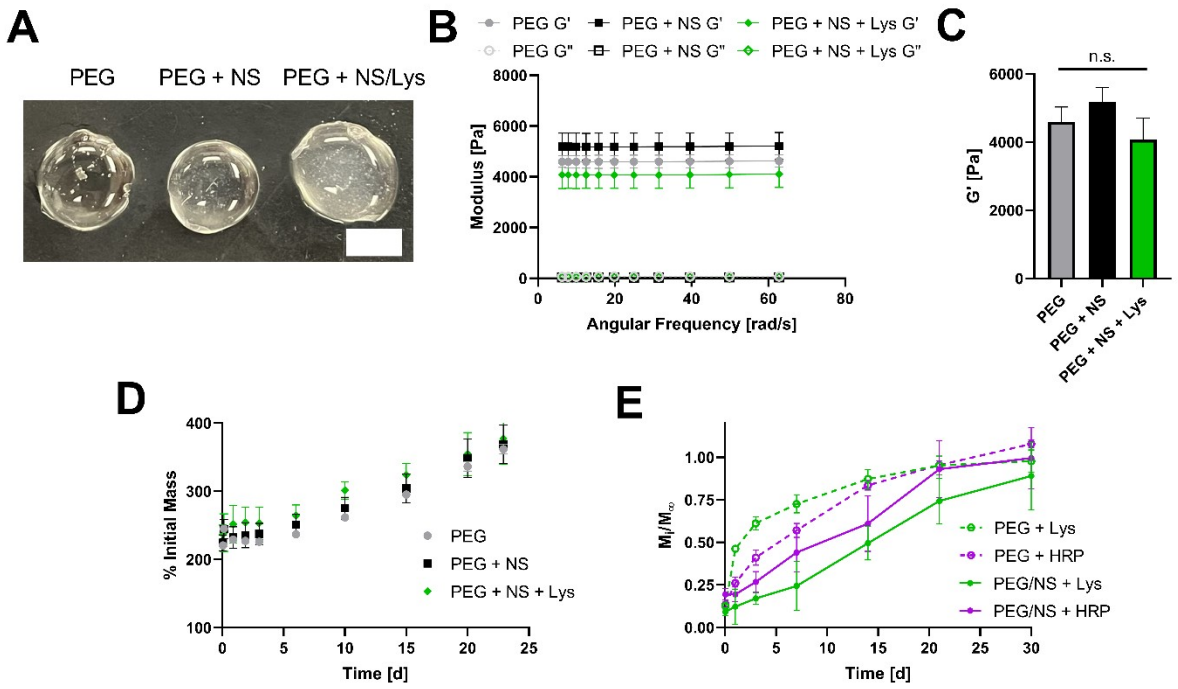

Supplemental Figure S8: A. Macroscopic images of hydrogels formed in the absence and presence of Lys and NS. Scale bar represents 5 mm. **B-C.** Measured storage modulus, *G'* and loss modulus, *G"*, or hydrogels formed in the absence and presence of Lys and NS. **D.** Measured swelling of hydrogels as a function of time, where initial mass was the mass immediately following fabrication. Measured swelling percentages are all > 200% due to initial swelling from the fabricated hydrogel to reach its equilibrium swelling in ~2 h. **E.** Release kinetics of 1 mg/mL Lys or HRP from PEG-only (dashed lines) and PEG + 1 mg/mL NS hydrogels (solid lines).

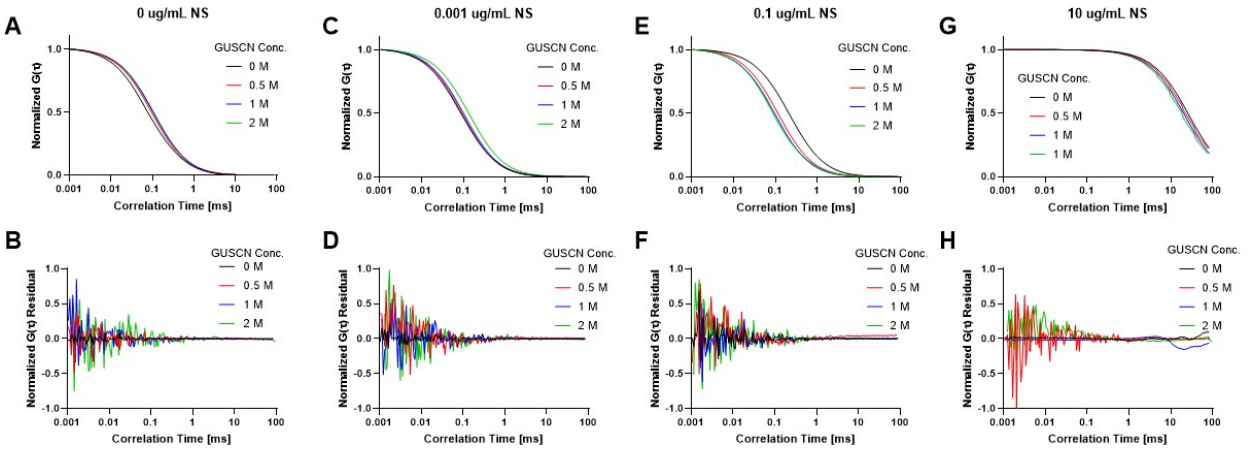

Supplemental Figure S9: Normalized autocorrelation curves of Atto-RNase A in the presence of varying concentrations of GUSCN and NS concentrations of 0 µg/mL (**A**, **B**), 0.001 µg/mL (**C, D**), 0.1 µg/mL (**E, F**), and 10 µg/mL (**G, H**).